NASA TECHNICAL MEMORANDUM

NASA TM X-2149

NASA TM X-2149

INSTRUMENTATION AND DROP-TESTING TECHNIQUES FOR INVESTIGATING FLIGHT VEHICLES AND PERSONNEL PROTECTIVE SYSTEMS

by

Richard Carpenter and Milton O. Thompson

Flight Research Center

and

Joseph H. Bowers

Northrop Corporation
Field Team at Flight Research Center

NATIONAL AERONAUTICS AND SPACE ADMINISTRATION • WASHINGTON, D. C. • JANUARY 1971

1. Report No.	2. Government Accession No.	3. Recipient's Catalog No.
NASA TM X-2149		

4. Title and Subtitle	5. Report Date
INSTRUMENTATION AND DROP-TESTING TECHNIQUES FOR INVESTIGATING FLIGHT VEHICLES AND PERSONNEL PROTECTIVE SYSTEMS	January 1971
	6. Performing Organization Code
7. Author(s) Richard Carpenter and Milton O. Thompson, Flight Research Center, Joseph H. Bowers, Northrop Corporation, Field Team at Flight Research Center	8. Performing Organization Report No. H-621
9. Performing Organization Name and Address NASA Flight Research Center P. O. Box 273 Edwards, California 93523	10. Work Unit No. 127-49-06-02-24
	11. Contract or Grant No.
12. Sponsoring Agency Name and Address National Aeronautics and Space Administration Washington, D. C. 20546	13. Type of Report and Period Covered Technical Memorandum
	14. Sponsoring Agency Code

15. Supplementary Notes

16. Abstract

A vehicle and flight systems dynamic impact laboratory, with appropriate instrumentation, was constructed recently at the NASA Flight Research Center. The purpose of the laboratory is to investigate energy-absorbing characteristics of various flight vehicle configurations and personnel protection and restraint systems during low-energy impacting. The laboratory was designed to permit investigation of a large range of horizontal and vertical impact velocities that would occur in low-level crash situations. It has provided acquisition of dynamic structural data on both vehicle configurations and personnel restraint systems.

17. Key Words (Suggested by Author(s))	18. Distribution Statement
Crash testing - Air vehicles	Unclassified - Unlimited

19. Security Classif. (of this report)	20. Security Classif. (of this page)	21. No. of Pages	22. Price*
Unclassified	Unclassified	18	$3.00

*For sale by the National Technical Information Service, Springfield, Virginia 22151

INSTRUMENTATION AND DROP-TESTING TECHNIQUES FOR INVESTIGATING FLIGHT VEHICLES AND PERSONNEL PROTECTIVE SYSTEMS

By Richard Carpenter and Milton O. Thompson
Flight Research Center

and

Joseph H. Bowers
Northrop Corporation
Field Team at Flight Research Center

INTRODUCTION

Late in 1968, plans were made to construct a dynamic impact laboratory capable of evaluating shock absorption and attenuating structural characteristics of vehicles and associated personnel support systems being investigated at the NASA Flight Research Center, Edwards, Calif. This laboratory was designed and constructed to simulate low-level crash conditions on a dry lakebed. It differs from other impact facilities (refs. 1 to 7) in that combinations of vertical and horizontal impact velocities may be programed together with a large range of specimen attitudes (yaw, pitch, and roll). These features make it possible to investigate dynamic behavior during abrupt external deceleration that simulates actual low-level crash conditions (refs. 8 and 9).

The dynamic impact laboratory, its instrumentation, and the drop-testing technique are described in this report.

SYMBOLS

Symbol terminology is consistent with that of Gell (ref. 10).

B, M	coefficients used to convert counts to g units
$B_{X'}, B_{Y'}, B_{Z'}$	coefficients used to convert counts to g units in X', Y', and Z' axes
C_k	average number of counts on each of the five calibration steps
$C_{X'}, C_{Y'}, C_{Z'}$	axial acceleration measurement in digitized counts, g units
$\bar{C}$	average number of counts for the five steps (eq. (5))

G	absolute magnitude of the acceleration vector sum, g units
G_f	acceleration magnitude at time T_f, g units
G_{kj}	each k-th calibration value typically in five steps, from -50g to 50g
G_o	acceleration magnitude at time T_o, g units
$\vec{G}_X, \vec{G}_Y, \vec{G}_Z$	axially measured acceleration vectors relative to laboratory axes, g units
$\vec{G}$	total measured acceleration vector, g units (See adjacent sketch.)
$\lvert\vec{G}\rvert = G$	
$\vec{G}_{X'}, \vec{G}_{Y'}, \vec{G}_{Z'}$	axially measured acceleration vectors, g units (See adjacent sketch.)
I/W	impulse per unit weight, lb-sec/lb (kg-sec/kg)
j, k	calibration steps
$M_{X'}, M_{Y'}, M_{Z'}$	coefficients used to convert counts to g units in X', Y', and Z' axes
n	number of calibration samples used for each channel of information
S_e	area under the acceleration curve and above the reference line G_o from T_o to T_e, g/sec
S_f	area under the acceleration curve and above the reference line G_o from T_o to T_f, g/sec
T	duration of impact, sec
T_e	time at end of impact interval, sec
T_f	time at end of onset interval, sec
T_o	time at initial impact, sec

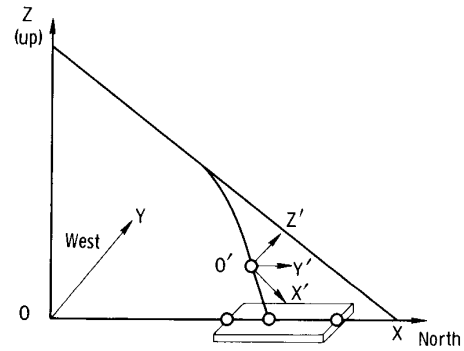

Right-hand cartesian coordinate system of laboratory (fixed)

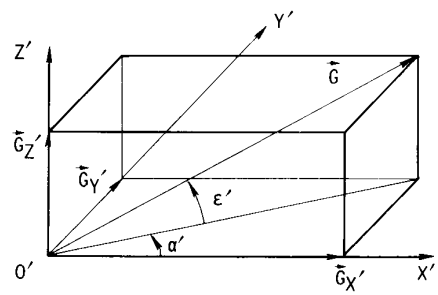

Right-hand cartesian coordinate system of accelerometer (moving)

t	time variable during impact, sec
X	longitudinal laboratory axis, positive forward
$\dot{X}$	impact velocity (X-direction), ft/sec (m/sec)
Y	lateral laboratory axis, positive left
Z	vertical laboratory axis, positive upward
$\dot{Z}$	impact velocity (Z-direction), ft/sec (m/sec)
$O \rightarrow X, Y, Z$	right-hand cartesian coordinate system of the laboratory (fixed) (See sketch, page 2.)
$O' \rightarrow X', Y', Z'$	moving-accelerometer coordinate system (See sketch, page 2.)
α', ϵ'	azimuth and elevation angles which define direction of the acceleration vector with respect to the accelerometer system, deg (See sketch, page 2.)
θ	pitch attitude of specimen during impact series, deg

DESCRIPTION OF APPARATUS

General Description

To accomplish the purposes of drop testing, the dynamic impact laboratory was constructed inside the Flight Research Center's High Temperature Loads Calibration Laboratory, a large, hangar-like facility. This arrangement not only shields experiments from the weather but provides temperature control throughout the year during dynamic impact testing. Figure 1 shows a typical test specimen at impact during a dynamic test in the laboratory, and figure 2 is a perspective drawing of the laboratory with a sketch of the coordinate system used.

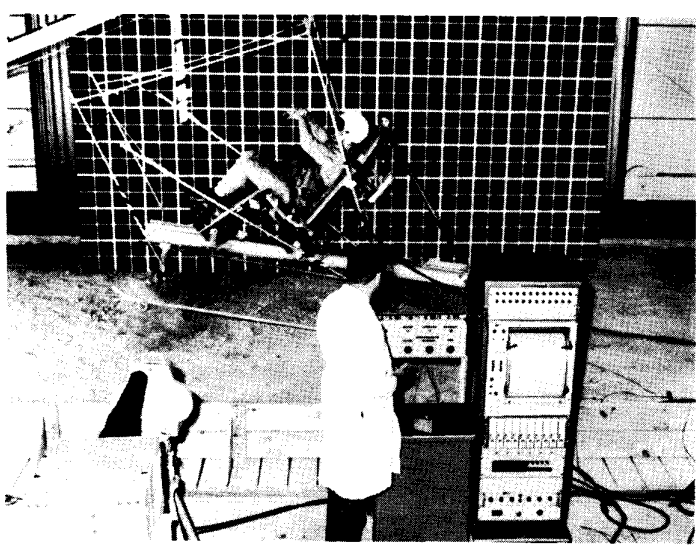

Figure 1. Typical test specimen at impact in the dynamic impact laboratory.

A performance envelope was calculated to show the various combinations of vertical and horizontal impact velocities that could be attained by a test specimen impacting on the test bed. The calculations took into account slight coefficient-of-friction drag

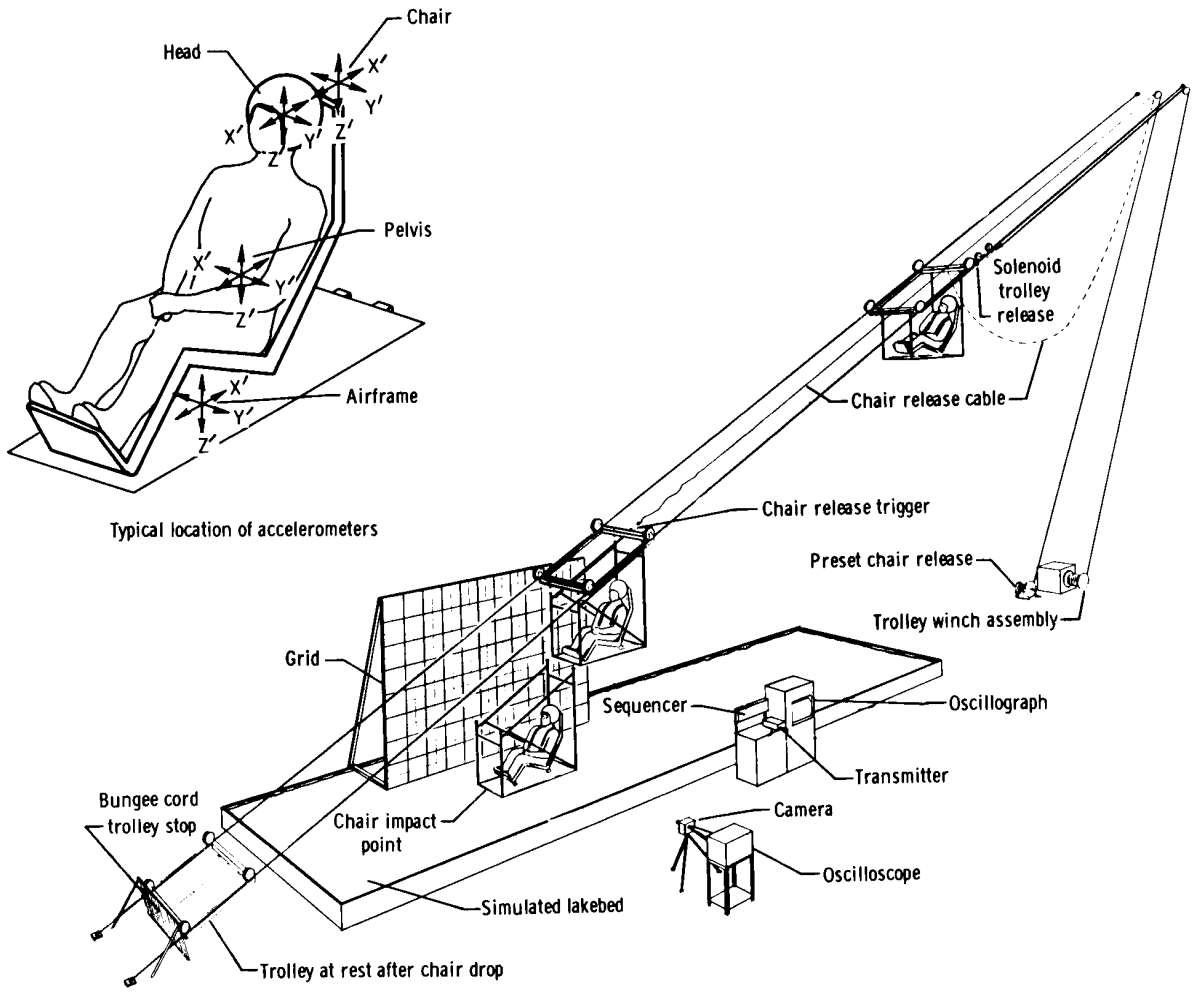

Figure 2. Perspective of dynamic impact laboratory and sketch of the coordinate system used.

loads determined empirically from limited laboratory measurements. Table 1 indicates a cross section of the obtainable performance values. As shown, vertical velocities ranging from approximately 48 feet/second (14.63 meters/second) to 0 feet/second are available with various combinations of horizontal velocities, depending upon the investigator's choice of trolley release point and specimen release point.

The dropping mechanism may be adjusted to provide a large range of roll, pitch, and yaw angles during impact. The monitoring instrumentation, data-handling procedures, and analytical techniques are configured specifically for use with the dynamic impact laboratory and were designed to permit the principal investigator to rapidly interpret and assess the results of each test drop. Instrumentation consists of 18 channels of accelerometers and force links, together with three high-speed motion picture cameras. The drop sequence is electronically controlled by appropriate time delays to allow completely automatic operation of any specific test drop; that is, a trolley is automatically released and rides down cable supports until the

TABLE 1. – SUMMARY OF THE DYNAMIC IMPACT LABORATORY VELOCITY PERFORMANCE ENVELOPE

[U. S. Customary Units]

Initial track displacement, ft	Release point, ft	X, drop, ft	Z, drop, ft	$\dot{X}$, ft/sec	$\dot{Z}$, ft/sec
0	0	0	35.7	0	-47.87
0	15.0	14.0	30.2	17.47	-44.57
15	15.0	14.0	30.2	0	-44.04
0	30.0	27.9	24.7	24.70	-41.01
15	30.0	27.9	24.7	17.47	-40.43
30	30.0	27.9	24.7	0	-39.84
0	45.0	41.9	19.2	30.25	-37.10
15	45.0	41.9	19.2	24.70	-36.46
30	45.0	41.9	19.2	17.47	-35.81
45	45.0	41.9	19.2	0	-35.15
50	50.0	46.5	17.4	0	-33.44
0	60.0	55.8	13.8	34.93	-32.74
15	60.0	55.8	13.8	30.25	-32.01
30	60.0	55.8	13.8	24.70	-31.26
45	60.0	55.8	13.8	17.47	-30.50
50	60.0	55.8	13.8	14.26	-30.24
60	60.0	55.8	13.8	0	-29.72
0	75.0	69.8	8.3	39.06	-27.69
15	75.0	69.8	8.3	34.93	-26.82
50	70.0	65.2	10.1	20.17	-26.67
60	70.0	65.2	10.1	14.26	-26.08
30	75.0	69.8	8.3	30.25	-25.93
70	70.0	65.2	10.1	0	-25.47
45	75.0	69.8	8.3	24.70	-25.01
50	80.0	74.5	6.4	24.70	-22.54
60	80.0	74.5	6.4	20.17	-21.83
0	90.0	83.8	2.8	42.78	-21.48
70	80.0	74.5	6.4	14.26	-21.10
15	90.0	83.8	2.8	39.06	-20.36
80	80.0	74.5	6.4	0	-20.34
30	90.0	83.8	2.8	34.93	-19.17
45	90.0	83.8	2.8	30.25	-17.90
80	85.0	79.1	4.6	10.08	-17.67
50	90.0	83.8	2.8	28.52	-17.45
60	90.0	83.8	2.8	24.70	-16.53
70	90.0	83.8	2.8	20.17	-15.55
80	90.0	83.8	2.8	14.26	-14.50
90	90.0	83.8	2.8	0	-13.38
90	92.0	85.6	2.1	6.38	-11.76
80	95.0	88.4	1.0	17.47	-10.43
90	94.0	87.5	1.3	9.02	-9.88
95	95.0	88.4	1.0	0	-7.85
90	96.0	89.4	.6	11.05	-7.55
95	96.0	89.4	.6	4.51	-6.42
90	97.0	90.3	.2	11.93	-6.05
95	97.0	90.3	.2	6.38	-4.57

TABLE 1. – SUMMARY OF THE DYNAMIC IMPACT LABORATORY VELOCITY PERFORMANCE ENVELOPE

[SI Units]

Initial track displacement, m	Release point, m	X, drop, m	Z, drop, m	$\dot{X}$, m/sec	$\dot{Z}$, m/sec
0	0	0	10.88	0	-14.59
0	4.57	4.27	9.20	5.32	-13.58
4.57	4.57	4.27	9.20	0	-13.42
0	9.14	8.50	7.53	7.53	-12.50
4.57	9.14	8.50	7.53	5.32	-12.32
9.14	9.14	8.50	7.53	0	-12.14
0	13.72	12.77	5.85	9.22	-11.30
4.57	13.72	12.77	5.85	7.53	-11.11
9.14	13.72	12.77	5.85	5.32	-10.91
13.72	13.72	12.77	5.85	0	-10.71
15.24	15.24	14.17	5.30	0	-10.19
0	18.29	17.01	4.21	10.65	-9.98
4.57	18.29	17.01	4.21	9.22	-9.76
9.14	18.29	17.01	4.21	7.53	-9.53
13.72	18.29	17.01	4.21	5.32	-9.30
15.24	18.29	17.01	4.21	4.35	-9.22
18.29	18.29	17.01	4.21	0	-9.06
0	22.86	21.28	2.53	11.91	-8.44
4.57	22.86	21.28	2.53	10.65	-8.17
15.24	21.34	19.87	3.08	6.15	-8.13
18.29	21.34	19.87	3.08	4.35	-7.95
9.14	22.86	21.28	2.53	9.22	-7.90
21.34	21.34	19.87	3.08	0	-7.76
13.72	22.86	21.28	2.53	7.53	-7.62
15.24	24.38	22.71	1.95	7.53	-6.87
18.29	24.38	22.71	1.95	6.15	-6.65
0	27.43	25.54	.85	13.04	-6.55
21.34	24.38	22.71	1.95	4.35	-6.43
4.57	27.43	25.54	.85	11.91	-6.21
24.38	24.38	22.71	1.95	0	-6.20
9.14	27.43	25.54	.85	10.65	-5.84
13.72	27.43	25.54	.85	9.22	-5.46
24.38	25.91	24.11	1.40	3.07	-5.39
15.24	27.43	25.54	.85	8.69	-5.32
18.29	27.43	25.54	.85	7.53	-5.04
21.34	27.43	25.54	.85	6.15	-4.74
24.38	27.43	25.54	.85	4.35	-4.42
27.43	27.43	25.54	.85	0	-4.08
27.43	28.04	26.09	.64	1.94	-3.58
24.38	28.96	26.94	.30	5.32	-3.18
27.43	28.65	26.67	.40	2.75	-3.01
28.96	28.96	26.94	.30	0	-2.39
27.43	29.26	27.25	.18	3.37	-2.30
28.96	29.26	27.25	.18	1.37	-1.96
27.43	29.57	27.52	.06	3.64	-1.84
28.96	29.57	27.52	.06	1.94	-1.39

appropriate horizontal and vertical velocities are achieved. At that time the test specimen is sequenced to free fall to a predetermined impact condition. High-speed cameras are energized to record the event in three dimensions at the appropriate times. The acceleration data are simultaneously recorded on the photographic film and telemetered to a ground station where the information is recorded on analog tape in a format compatible with analog-to-digital conversion equipment for later computer reduction and analysis. The projection of the accelerometer data directly on the subject area of each photographic frame allows the investigator to rapidly assess, during slow playback of the developed film, the onset and peak g levels at preselected points on the structure being investigated while simultaneously observing the actual event in very slow motion. Computer programs provide onset rates, peak acceleration levels, rotational angles, and vector sums as determined from three-axis accelerometers.

Detailed Description

To obtain vertical and horizontal impact velocities or any combination of these velocities, two cables were fitted near the top of a large room and stretched diagonally to the floor. The upper end of the cables is 38 feet (11.58 meters) high and extends a horizontal distance of 100 feet (30.48 meters). The cables are 6 feet (1.83 meters) apart and marked at 1-foot (0.30-meter) increments, with every 5- and 10-foot (1.52- and 3.05-meter) mark of a different color. Such markings allow the operator to accurately locate the test specimen in order to achieve the combination of horizontal and vertical impact velocities desired. The cables are anchored in the floor to sunken rail tracks and, if necessary, may be repositioned to change the slope. The 5/8-inch (1.59-centimeter) cables are stretched by turnbuckles equipped with bonded strain gages to monitor the tension. To provide standardization through a series of tests, the cables are stretched to 5000 pounds (2270 kilograms) tension just prior to a drop. The constant cable tension prevents changes in vertical height due to cable sag and maintains a relatively constant coefficient of friction between the cable and the trolley carrying the test specimen.

Two specimen-carrying trolleys are available: a one-cable trolley with two wheels, used for lighter weight specimens (< 500 lb (< 227 kg)), and a two-cable trolley with four wheels, used for heavier specimens (< 1200 lb (< 545 kg)). The trolleys are positioned along the cable by a 1/4-inch (0.64-centimeter) cable and pulleys placed in the same plane as the cable run.

A 3.5-horsepower, two-way, variable-speed winch is used to draw the trolleys. The winch is remotely controlled from the main operator's position. Each trolley is equipped with a disconnect that allows a two-point attachment to a test specimen for the one-cable trolley and a four-point attachment for the two-cable trolley. Figure 3 illustrates the mechanism used to achieve simultaneous release of the disconnect apparatus. The direct mechanical linkage together with the rigid framework that attaches the test specimen to the trolley provides a means of orienting the specimens for ±30° of pitch and 0 to 35° of either right or left roll and simultaneously preventing the specimen from swinging or swaying during the trolley run down the cable to the release point.

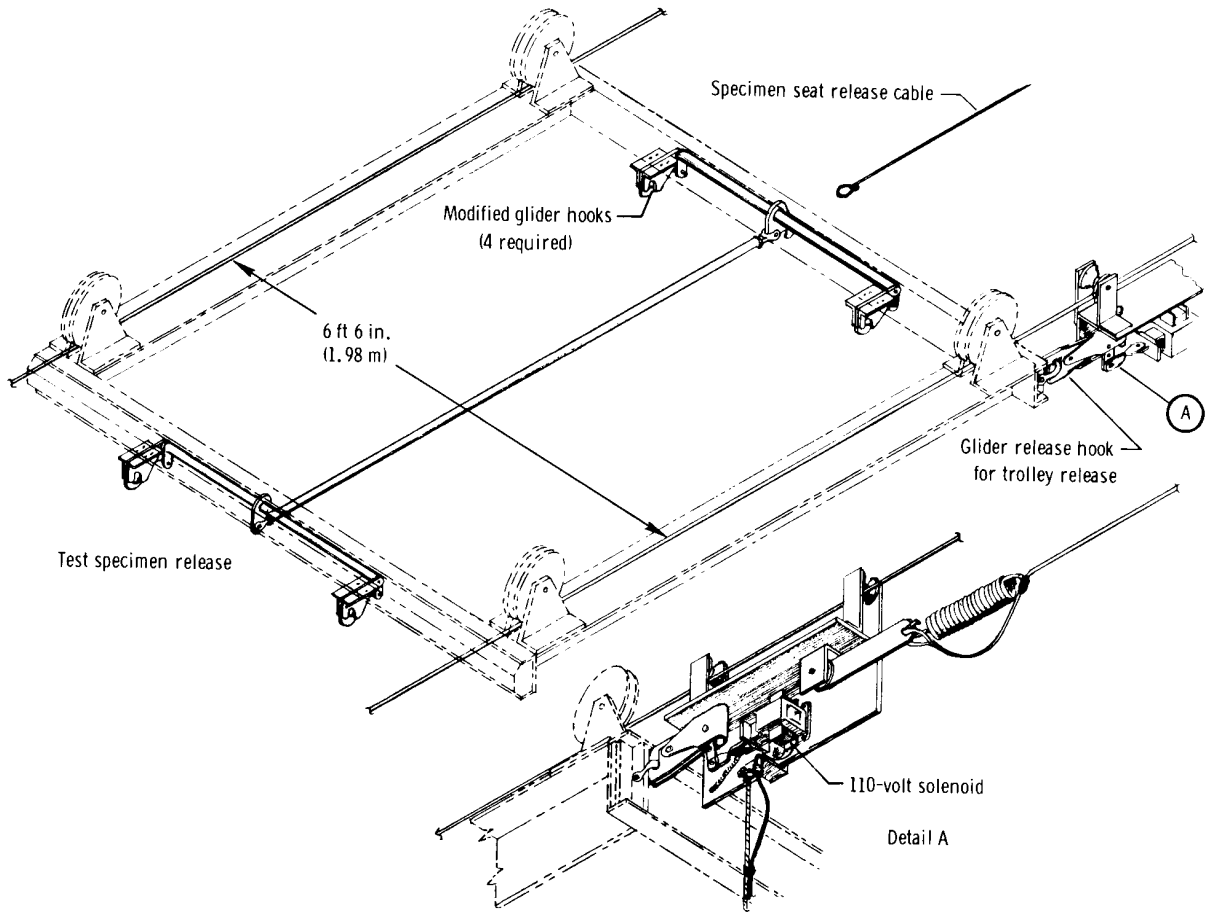

Figure 3. Trolley release mechanism.

The distance of the trolley run down the cable and the release point on the cable determine the vertical and horizontal impact velocities to be achieved. The trolley release is electronically sequenced to coincide with the energizing of high-speed cameras, timing lights, and other instrumentation. For reliability and standardization, the specimen-release point is actuated by a special lanyard that triggers the disconnect apparatus. Figure 3 shows the electronic and lanyard release scheme. A small traveling release fitted with a glider release hook energized by an electrical solenoid is connected to the trolleys to act as the interface for positioning and electronically releasing either trolley, as shown in view A.

After the specimen is released, the trolley continues to roll down the cable and impacts a bungee cord barrier. The trolley is constructed so that the impact loads it receives place its longitudinal members in a direct line for compression and the energy from the high impact loads is dissipated by the bungee as it bounces the trolley back and forth on the cable supports. The bungee cable barrier is equipped with a personnel shield in the event a cable should snap.

The drop test-bed simulates the dry lakebed conditions of Rogers Dry Lake, adjacent to the Flight Research Center. The test-bed, which is 25 feet (7.62 meters) wide and 50 feet (15.24 meters) long, contains dry lakebed dirt to a depth of 12 inches (30.48 centimeters). Through a combination of compacting, water soaking, and vibration rolling, the test-bed was brought within 20 percent of the penetrability and to within 8 percent of the compressibility of the dry lakebed. Penetrability and compressibility were determined by the use of a sharp spike and a shotput ball dropped from a height of 10 feet (3.05 meters). Thirty tests of this nature were made under dry conditions in various areas of the lakebed, and the results were compared with results from similar tests on the test-bed.

INSTRUMENTATION

The dynamic impact laboratory has the necessary instrumentation to fully monitor the dynamic characteristics of a specimen during impact. The layout of the instrumentation is shown in figure 4. The instrumentation includes high-speed cameras in each of the three planes and a wide assortment of accelerometers. The instrumentation is designed to provide the investigator with on-line data immediately after each drop test. The acceleration and position data are placed in storage on magnetic tapes for use with computer programs. Programs have been written to provide the investigator with hard-copy listings of onset rates, peak-to-peak g values, rotational angles, and vector sums.

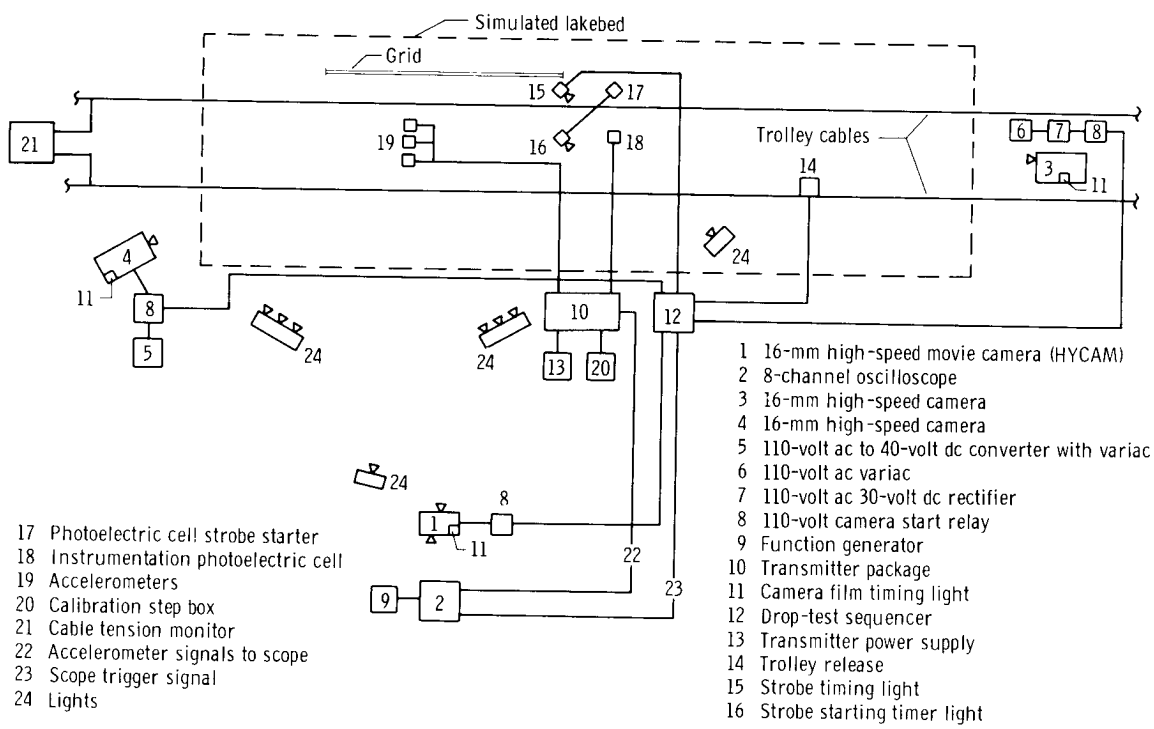

Figure 4. Instrumentation layout.

High-Speed Cameras

A typical camera placement relative to the test-bed is diagramed in figure 4. Each camera is electronically sequenced to reach the necessary speed to photograph the portion of the test for which the camera is intended. As a specimen travels from right to left, one camera (4) photographs the front of the specimen while another camera (3) photographs the back. The side camera (1) is usually located at the center point of impact to photograph the side of the specimen. The other two cameras have capabilities of up to 2000 frames per second in color, and each is equipped with a timing event marker. The HYCAM camera (1) was modified to allow simultaneous exposure of the film from both sides, which permits the camera to photograph the specimen at high speeds (100 to 11,000 frames per second) and to simultaneously record oscillograph tracings displayed by the oscilloscope screen. This arrangement allows the investigator to rapidly assess the dynamic characteristics of the specimen being impacted. During one test sequence, for example, a capsule mounted with an energy-absorbing seat and a dummy were instrumented with three-axis accelerometers. During impact the exact attenuation levels between the capsule, the seat, and the dummy were obvious to the investigator by viewing the film. This feature made it possible to quickly assess energy-absorption characteristics designed and built into the seat as well as the natural damping characteristics of the structures involved.

The modified HYCAM camera is constructed in a manner which permits replacement of the eyepiece with a 50-millimeter lens that may be focused on an oscilloscope face. To achieve proper lighting contrasts between the specimen area and the acceleration traces being photographed, 22 kilowatts of light were required on the specimen area and a black tube was used to join the oscilloscope to the camera. In addition, the oscilloscope was specially equipped with a P-14 phosphorus screen to provide a quick decay time for the electron beam. The oscilloscope has eight channels and for this operation requires a very slow, remotely triggered, synchronized scan of 0.5 second and a vertical amplitude of 5 volts per centimeter.

As shown in figures 2 and 4, the grid was placed behind the specimen and thus accomplished two roles: a quantitative estimate of distance traveled in two planes and a quantitative evaluation of onset rates and peak-to-peak g levels. The onset rates and peak-to-peak g levels were determined from the oscillographic traces superimposed on the grid background, which was scaled so that each 6-inch (15.24-centimeter) grid line corresponded to an acceleration of 25g. Because the grid was placed behind the specimen, it was necessary to provide grid lines that were always visible to the observer. This was accomplished by placing reticle markings on the camera lens which allow the investigator to assess acceleration-trace excursions when the grid is obscured by the specimen.

Accelerometers

Accelerometers are available with ranges of ±10g peak-to-peak, ±50g peak-to-peak, ±150g peak-to-peak, and ±4500g peak-to-peak. All the accelerometers are miniaturized and have amplifiers integrated with the sensing element. Accelerometers at each location are always used in the three-axis configuration; the three-axis chassis were designed to allow easy mounting in difficult-to-reach locations. To facilitate standardization and ease of data reduction, all accelerometers have a high-level output signal of 0 to 5 volts peak-to-peak. This high-level signal may be paralleled simultaneously

for transmission to the transmitter, oscilloscopes, and high-frequency response oscillographs.

Also available is an instrumented dummy with three axes of acceleration, in the head, thorax, and pelvic regions. The dummy is also equipped with a position potentiometer in the chest cavity to provide the investigator with chest deflection values from which forces may be calculated. The dummy is a fully articulated, anthropomorphic type of a 95 percentile; however, the weight of the dummy may be varied to a 60 percentile.

Telemetry

The acceleration and position data may be telemetered from the dynamic impact laboratory, as shown in figure 5, to a ground station (ref. 11) and be formatted for analog-to-digital conversion to allow computer processing. The telemetry system, which is in a miniaturized flight-rated configuration, provides standard IRIG channels 1 through 18 plus a voice channel. This telemetry may be used in the dynamic impact laboratory or in flight.

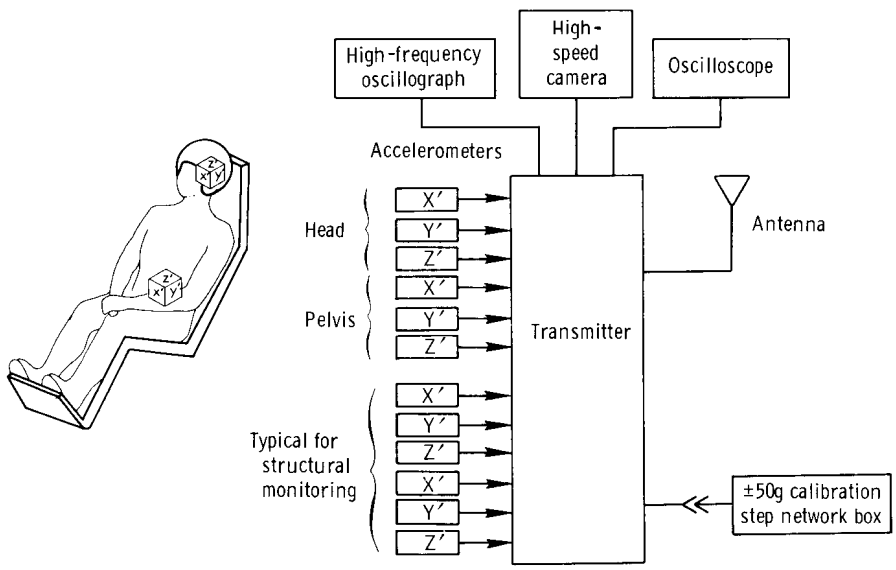

Figure 5. Typical specimen on instrumentation interface.

The telemetry transmitter is a flight-rated package capable of accepting low-level signals of 10 millivolts or high-level signals of 0 to 5 volts. The telemetered signals are radioed to a remote data-acquisition site containing a primary telemetry receiver and a backup receiver (fig. 6). The signals are then fed through standard IRIG discriminators in which the intelligence is demodulated and routed simultaneously to high-frequency oscillographs and to analog magnetic-tape recorders. Since the standard IRIG channels are limited in frequency, especially in the low-numbered channels, a data-acquisition system at the test site is available for use when high-frequency data are encountered. The on-site data-acquisition system includes digital voltmeter readouts, high-speed oscillographs, and a magnetic-tape recorder.

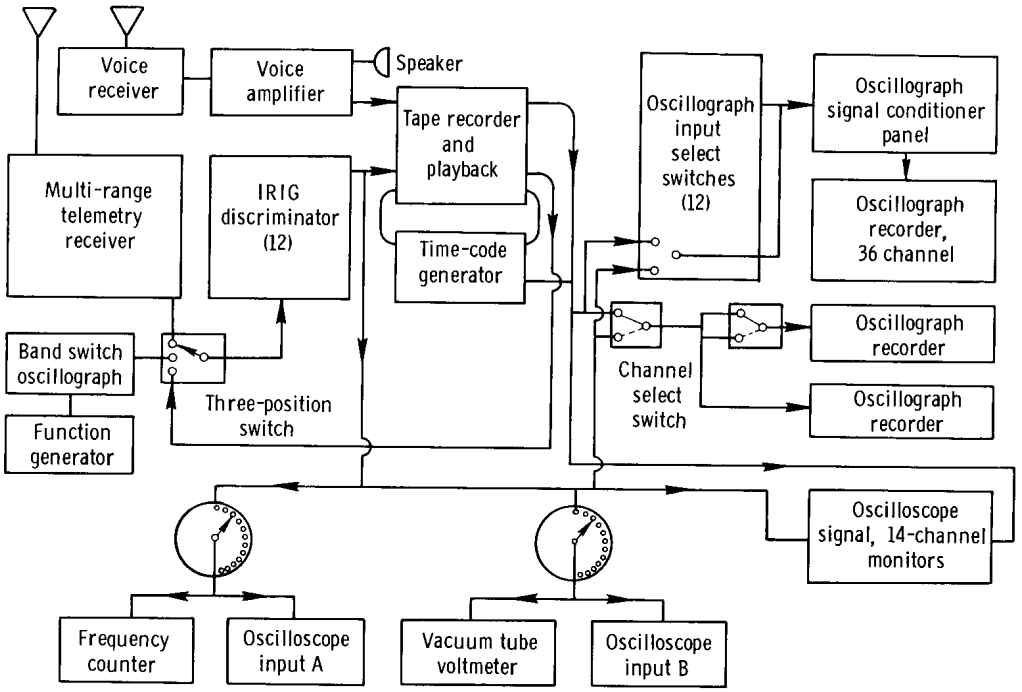

Figure 6. Electrical schematic of receiving and data-handling station.

ANALOG CALIBRATION

Calibration data are acquired before and after each test in two steps. The first step involves placing voltages corresponding to g levels on the oscilloscope being photographed by the high-speed HYCAM camera. This provides a calibration for the accelerometer tracings that are photographed simultaneously with the test specimen. The other calibration consists of placing voltages corresponding to the range of g values to be recorded by both the ground station and the on-site high-frequency data-acquisition system. An automatically sequenced calibration system was designed and constructed to place voltage steps corresponding to the average value of all types of accelerations at their appropriate levels of measurement.

Before any testing sequence, all accelerometers are dynamically and statically calibrated by shake tables and a centrifuge, respectively. The calibration values are written into the computer program, and all data are corrected during analyses. The instrumentation system is maintained at a signal-to-noise ratio of 35 decibels for intelligence in the frequency range of 2 to 100 hertz.

DATA HANDLING AND REDUCTION

The optical data-conversion system in the Flight Research Center's Biodata Analyses Laboratory provides for measurements on oscillograms and high-speed photography film. As shown in figure 7, horizontal and vertical linear measurements and angular measurements for film reduction are fed through the accumulator to the summary punch. The summary punch prepares cards which are input to various

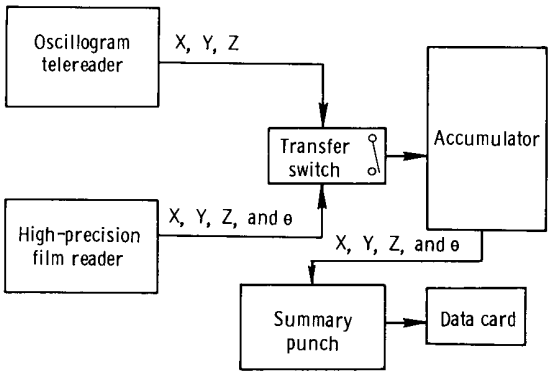

Figure 7. Data-handling system for oscillographic and film data.

IBM 360 computer programs. The optical data-conversion system is modular in design to permit easy future additions or changes of key components. Basic X-Y coordinate display is provided through the use of crosshairs, and a device to measure angles is attached. Readout of the coordinates is to the nearest 0.001 inch (0.025 millimeter), and of the angles, to 0.1°. This allows data to be reduced from oscillograph and film measurements made during the drop tests. From X and Y or Z measurements, position, velocity, acceleration, rate of onset, vehicle pitch or roll angles, or head angular accelerations are computed during impact of drop test specimens. Thus, a means is provided for converting pictorial data such as high-speed photographs into a format amenable to computer processing.

Since computer programs are required to eliminate the vast amount of hand calculations, the analog tapes for the acceleration and position data are recorded or handled in a manner that allows analog-to-digital conversion. The analog tapes are standard IRIG 1-inch (2.54-centimeter), 14-channel tapes recorded at 60 inches/second (1.52 meters/second). Routinely, there are 12 channels of accelerometer data, 1 composite channel, and 1 channel of IRIG-B time code.

The sampling rate required to maintain adequate frequency resolution is 2000 samples per second. A bit rate of 90 kilohertz (commutation scheme) together with a typical channel layout format is shown in table 2.

TABLE 2. – DIGITAL COMMUTATION SCHEME FOR TYPICAL CHANNEL FORMAT

[Bit rate = 90 kHz]

	1	2	3	4	5	6	7	8
1	3	4	5	6	7	8	9	10
2	11	12	13	14				
3					3	4	5	6
4	7	8	9	10	11	12	13	14
5								
6	3	4	5	6	7	8	9	10
7	11	12	13	14				
8					3	4	5	6
9	7	8	9	10	11	12	13	14
10						Time words		Sync word

The data-handling system will digitize ±2.5 volts representing a count range of 0 to 511_{10}. The ±50g output voltage on an analog tape is ±1.000 volt, ±1 percent (±40-percent frequency deviation). Maximum voltages of ±1.414 volts correspond to ±70.7g. The equipment used and the data flow are illustrated in figure 8. A process was developed to verify that the entire analog-to-digital system is set up and functioning properly. The process consists of digitizing a test tape with known voltages on each channel and printing the results along with the range of expected values for each channel. If a discrepancy is noted, the problem is corrected and the entire process is repeated until all values fall within the expected range.

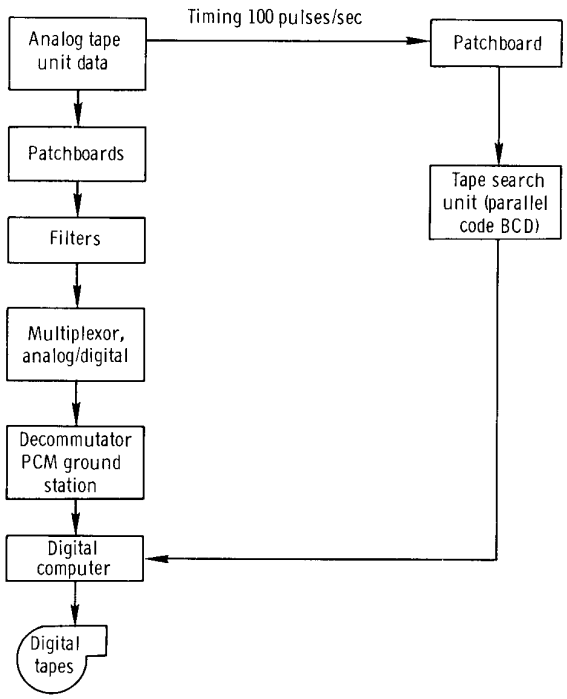

Figure 8. Analog-to-digital-conversion equipment configuration.

The entire digitizing process is under the control of a digital computer program. The program calls instructions to the operator to be typed, checks the status of the digital tapes, accepts starting and stopping times typed by the operator, accepts acceleration and force-link data and time words, and causes digitizing to start when starting time is found and to stop when stopping time is found. During actual digitizing, the program is signaled by an interrupt each time a frame of data enters the computer. The program combines the data with a time word, collects 12 frames of data, and writes them on the output tape in the form of a record. This process results in IBM 360 compatible tapes with one file for pretest calibrations, one file for impact data, and another file for post-test calibrations.

AUTOMATIC DIGITAL DATA PROCESSING

Data from the dynamic impact laboratory are automatically processed to provide parameters of interest to the principal investigator in the form of hard-copy outputs from the computer. The digitized data counts are converted to calibrated acceleration values by using the following equations:

$$G_X' = M_X'C_X' + B_X' \tag{1}$$

$$G_Y' = M_Y'C_Y' + B_Y' \tag{2}$$

$$G_Z' = M_Z'C_Z' + B_Z' \tag{3}$$

where C_X', C_Y', and C_Z' are in the digital count range of 0 to 511. The coefficients M_X', M_Y', M_Z' and B_X', B_Y', B_Z' are derived from a least-squares fit of the pre-test calibrations in the following manner:

$$C_k = \frac{1}{n} \sum_{j=1}^{n} G_{kj} \tag{4}$$

$$\bar{C} = \frac{1}{5} \sum_{k=1}^{5} C_k \tag{5}$$

where $k = 1 \ldots 5$ corresponds to the calibration steps (for example, G_{kj} = -50g, -25g, 0 g, 25g, 50g), C_k is the average number of digitized counts for the k-th step, n is the number of samples used from the k-th step, and $\bar{C}$ is the average number of counts for the five steps. These values are used in the following manner:

$$M = \sum_{k-1}^{5} \frac{G_{kj}(C_k - \bar{C})}{\sum_{k=1}^{5}} (C_k - \bar{C})^2 \tag{6}$$

$$B = -M\bar{C} \tag{7}$$

After the correction is made for the calibration, the magnitude of $\vec{G}$ is calculated by using the expression

$$G = |\vec{G}| = \left(G_X'^2 + G_Y'^2 + G_Z'^2 \right)^{1/2} \tag{8}*$$

and the direction of $\vec{G}$ from the expressions

$$\alpha' = \text{arc tan} \frac{G_Y'}{G_X'} \text{ (azimuth)} \tag{9}*$$

and

$$\epsilon' = \text{arc tan} \frac{G_Z'}{\left(G_X'^2 + G_Y'^2\right)^{1/2}} \text{ (elevation)} \tag{10}*$$

In addition, the time interval of the impact defined as

$$T = T_e - T_o \text{ (fig. 9)} \tag{11}*$$

*Equation numbers with asterisks denote those values printed out by the computer.

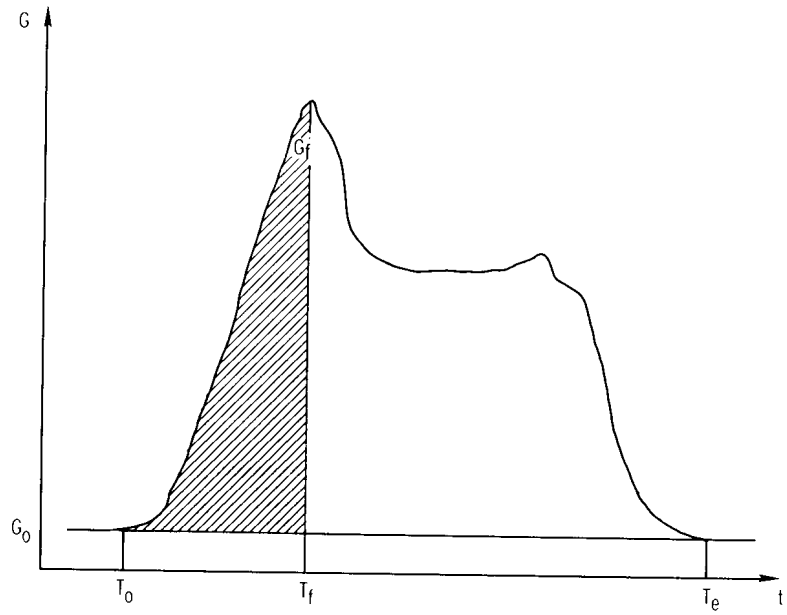

Figure 9. Acceleration energy wave form.

is printed out together with the onset values of each impact peak defined as the average slope of the G curve in figure 9 from T_o to T_f in g/second calculated as follows:

$$\text{Rates of onset} = \frac{(G_f)^2}{(2S_f)} \text{ g/second} \qquad (12)^*$$

For each measurement station, the value of impulse per unit weight or total energy is computed as

$$\frac{I}{W} = \int_{T_o}^{T_e} G dt = S_e \text{ (fig. 9)} \qquad (13)^*$$

Thus, $\vec{G}$ magnitude and direction, impact areas (total energy), and impact velocities are computer hard-copy outputs. In addition, the angle of each directional vector is available to compute rotational angles of an instrumented specimen.

Figures 10 and 11 are samples of hard-copy output. Figure 10 presents onset and total energy values in terms of lb-sec/lb (kg-sec/kg) together with the interval times of impact, and figure 11 is a digital printout of the vector sums of a three-axis accelerometer at different stations for a typical specimen impact test.

Station number	Start of event interval, T_o,				End of onset interval, T_f,				End of event interval, T_e,				Rate of onset T_o through T_f, g/sec	Impact duration, T, msec	Impulse per unit weight, I/W,	
	hr	min	sec	msec	hr	min	sec	msec	hr	min	sec	msec			lb-sec/lb	kg-sec/kg
Head 1	16	34	19	530	16	34	19	682	16	34	19	698	186.5	168	1.43	0.64
Pelvis 2	16	34	19	547	16	34	19	612	16	34	19	656	462.2	109	0.78	0.35
Seat 3	16	34	19	556	16	34	19	590	16	34	19	658	2077.8	102	1.52	0.69
Vehicle 4	16	34	19	554	16	34	19	588	16	34	19	638	2060.1	84	0.96	0.44

Figure 10. Example of automatic data printout.

*Equation numbers with asterisks denote those values printed out by the computer.

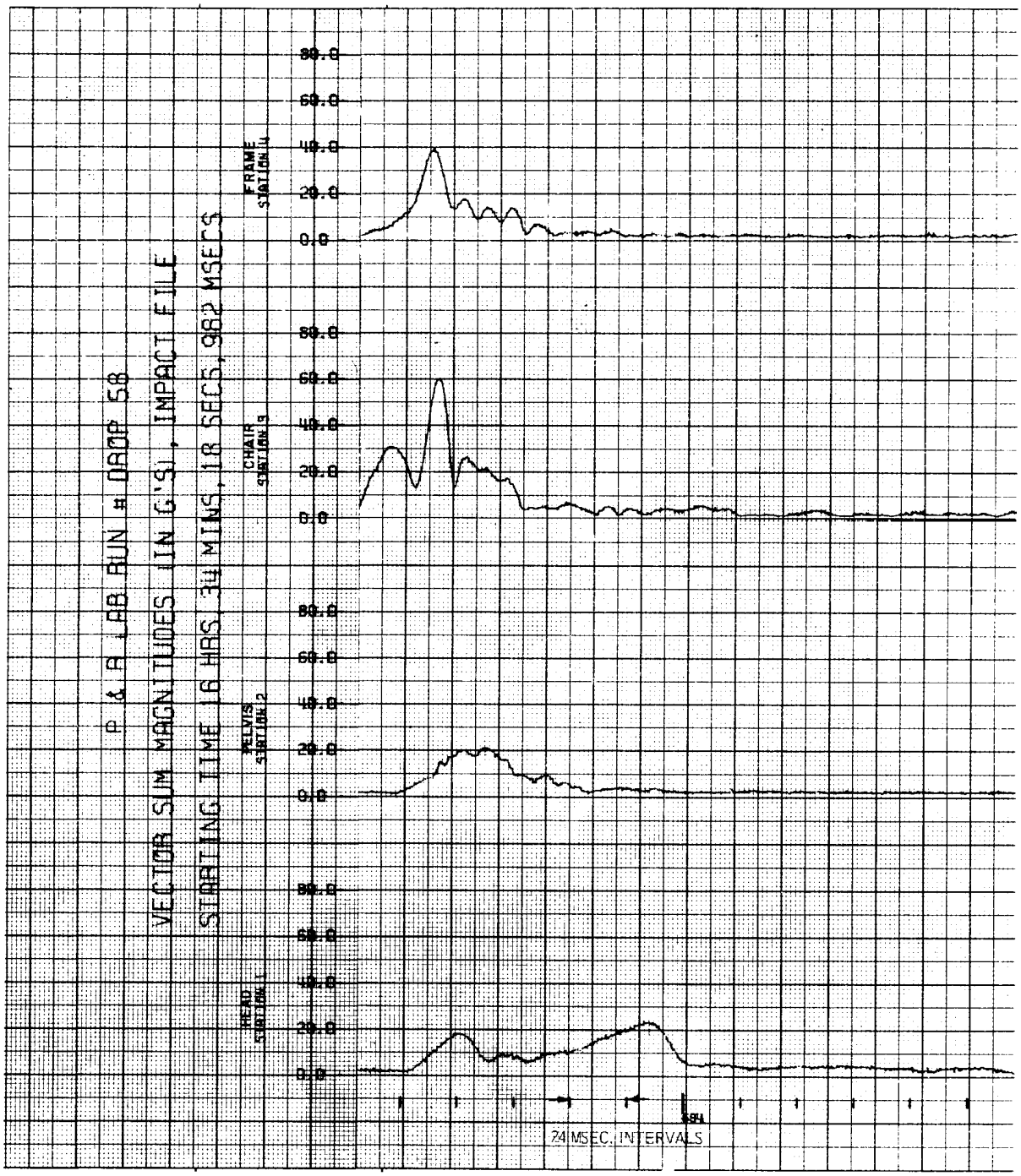

Figure 11. Accelerometer vector sums.

Flight Research Center,
National Aeronautics and Space Administration,
Edwards, Calif., July 8, 1970.

REFERENCES

1. Stapp, J. P.; Mosely, J. D.; Lombard, C. F.; and Nelson, G. A.: Analysis and Biodynamics of Selected Rocket-Sled Experiments. Part 1. Biodynamics of Maximal Decelerations. (Contract No. AF41(609)-2317), USAF School of Aerospace Medicine. Aerospace Med. Div. (AFSC), Brooks Air Force Base, Tex., July 1964.

2. Winquist, Paul G.; Stumm, Philip W.; and Hansen, Robin: Crash Injury Experiments With the Monorail Decelerator. Tech. Rep. No. AFFTC 53-7, Air Force Flight Test Center, U.S. Air Force, April 27, 1953. (Available from ASTIA as AD 16297.)

3. von Gierke, Henning, E.; and Steinmetz, Eugene: Motion Devices for Linear and Angular Oscillation and for Abrupt Acceleration Studies on Human Subjects (Impact). Publication 903, National Academy of Sciences--National Research Council. 1961. (Available from ASTIA as AD 266 078.)

4. Hawkins, Willard R.; and Hessberg, Rufus R.: USAF Impact Acceleration Program and Facilities. Symposium on Impact Acceleration Stress, Pub. 977, Nat. Acad. Sci.--Nat. Res. Council, 1962, pp. 313-322.

5. Stapp, John P.; and Blount, Wilbur C.: Effects of Mechanical Force on Living Tissue. III. A Compressed Air Catapult for High Impact Forces. J. Aviation Medicine, vol. 28, no. 3, June, 1957, pp. 281-290.

6. Lewis, Sidney T.; and Stapp, John P.: Experiments Conducted on a Swing Device for Determining Human Tolerance to Lap Belt Type Decelerations. AFMDC TN 57-1 (ASTIA No. AD 135005), Air Force Missile Dev. Center, Dec. 1957.

7. Brooks, George W.; and Carden, Huey D.: A Versatile Drop Test Procedure for the Simulation of Impact Environments. Noise Control, vol. 7, no. 5, Sept.-Oct. 1961, pp. 4-8.

8. Taylor, Ellis R.: Biodynamics: Past, Present and Future. Tec. Doc. Rep. No. ARL-TDR-63-10, U.S. Air Force, Mar. 1963. (Available from ASTIA as AD No. 402084.)

9. Turnbow, J. W.; Carroll, D. F.; Haley, J. L., Jr.; Reed, W. H.; Robertson, S. H.; and Weinberg, L. W. T.: Crash Survival Design Guide. USAAVLABS TR 67-22, Aviation Safety Eng. and Res. (Phoenix, Ariz.), July 1967. (Available from ASTIA as AD 656621.)

10. Gell, C. F.: Table of Equivalents for Acceleration Terminology. Aerospace Medicine, vol. 32, no. 12, Dec. 1961, pp. 1109-1111.

11. Zweizig, J. Rod; Kado, Raymond T.; Hanley, John; and Adey, W. Ross: The Design and Use of an FM/AM Radiotelemetry System for Multichannel Recording of Biological Data. IEEE Trans. on Bio-medical Engineering, vol. BME-14, no. 4, Oct. 1967, pp. 230-238.

NASA-Langley, 1970 — 14 H-621